

Study of Nonlinear Evolution of Single-Mode and Two-Bubble Interaction under Richtmyer-Meshkov Instability

O. Sadot,¹ L. Erez,¹ U. Alon,^{3,4} D. Oron,^{1,3} L. A. Levin,³ G. Erez,¹ G. Ben-Dor,² and D. Shvarts³

¹*Physics Department, Ben Gurion University of the Negev, Beer Sheva 84105, Israel*

²*Mechanical Engineering Department, Ben Gurion University of the Negev, Beer Sheva 84105, Israel*

³*Physics Department, Nuclear Research Center-Negev, Beer Sheva 84190, Israel*

⁴*Physics Department, Princeton University, Princeton, New Jersey 08540*

(Received 1 October 1997)

Shock-tube experiments were performed in order to verify recently developed theoretical models for the evolution of the shock-wave induced Richtmyer-Meshkov instability [Phys. Rev. Lett. **74**, 534 (1995)]. Single-mode bubble and spike evolution and two-bubble interaction in both early and late nonlinear stages were investigated in a $M \approx 1.3$ Air-to-SF₆ shock-tube experiment. Experimental results for the single-mode and two-bubble cases, showing distinct bubble and spike evolution, were found to be in very good agreement with the theoretical model prediction as well as numerical simulations, verifying the key elements of the bubble-merger model used for the prediction of the multimode bubble and spike front evolution. [S0031-9007(97)05261-7]

PACS numbers: 47.40.Nm, 52.35.Py

The instability mechanism which appears at an interface between two fluids of different densities accelerated by a shock wave, known as the Richtmyer-Meshkov (RM) instability, can give rise to turbulent mixing. The turbulent mixing caused by the RM instability is of great interest in inertial confinement fusion and astrophysics [1]. Recent theoretical work [2,3] has predicted the evolution of the instability through the late nonlinear stage. After the shock passage the interface can be described by an incompressible evolution of the flow field [2–5]. For a single-mode perturbation the instability can be described by a linear stage, during which the growth is characterized by a constant velocity, followed by a nonlinear stage [2–7]. The growth velocity reaches an asymptotic $1/t$ behavior [2,3,8–10].

An expansion of the flow equations to second order [2,4,8] yields $U(t) = U_0(1 \pm AkU_0t)$ (the minus sign is for the bubble, the plus for the spike), showing that the bubble velocity begins to decrease. A is the post-shock Atwood number, $k = 2\pi/\lambda$, and $U_0 = Ak\Delta Ua_0$ is the Richtmyer initial velocity, with ΔU the velocity jump after the incident shock passage and a_0 the post-shock amplitude. At late time, bubble velocities approach the same asymptotic form, $U_b = C\lambda/t$, where $C = 1/3\pi$ for $A \geq 0.5$ [2,3,9] and rises to about $C = 1/2\pi$ for low A 's [2,10]. The difference in the value of the coefficient C is attributed to the added mass effect [11]. The spikes at $A = 1$ initially accelerate, in accordance with the second-order expansion, and then saturate to a constant velocity. For $A < 1$ the spike velocity also rises initially and then begins to decrease, asymptotically going as [2] $U_s = [(1+A)/(1-A)](C\lambda/t)$.

We find that the whole evolution can be captured by a simple formula which fits the linear, early nonlinear, and asymptotic behavior of the bubble and spike evolution,

$$U(t) = U_0 \frac{1 + Bt}{1 + Dt + Et^2}, \quad (1)$$

with $B = U_0k$ for the bubble and for the spike, $D_{b/s} = (1 \pm A)U_0k$, and $E_{b/s} = [(1 \pm A)/(1 + A)] \times (1/2\pi C)U_0^2k^2$ with the plus sign for the bubble and the minus sign for the spike. This formula captures the linear and early nonlinear stages, up to second order, with the correct A dependence (except for $A \geq 0.9$ for the spike) and converges to the correct asymptotic limit with $C = 1/3\pi$ for $A \geq 0.5$ and $1/2\pi$ for $A \rightarrow 0$.

For the case of an initial multimode perturbation, two complementary approaches were introduced [12]: Fourier based mode-coupling model [8,12,13], suited mainly for early nonlinear evolution such as in the experiment of Ref. [14], and a statistical-mechanics bubble-competition model [2,15], suited mainly for derivation of scaling laws for the late time front growth. This latter model, which is an extension of the Sharp-Wheeler model [15], describes the behavior of an ensemble of rising bubbles, with overtake or merger interactions that lead to a continual increase of the dominant bubble size. In the model the 2D front is treated as an ensemble of bubbles arranged along a line, characterized by their wavelengths λ_i . Each of the bubbles rises with a velocity $U_i(\lambda_i)$ equal to the asymptotic velocity of a periodic array of bubbles with wavelength λ_i . The nonlinear interaction of bubbles of different wavelengths is described by a bubble-merger rate [2]. In this model, two adjacent bubbles of sizes λ_i and λ_{i+1} merge at a rate $\omega(\lambda_i, \lambda_{i+1})$, forming a new bubble of size $\lambda_i + \lambda_{i+1}$. This represents expansion of the surviving bubble to fill the space vacated by the bubble swept away from the front. The model was applied to derive the scaling laws for multimode classical RT and RM cases, resulting in new scaling laws for the bubble front evolution [2]. From the bubble front

evolution and the single-mode spike-to-bubble asymmetry it was possible to infer also the scaling laws for the spike front. It is therefore essential to provide the model with the three basic physical elements: the single-mode bubble evolution, the single-mode spike evolution, and the two-bubble interaction. These elements were provided in Ref. [2] using for $A = 1$ an incompressible potential flow model [3] and for $A < 1$ full numerical simulation together with simple buoyancy and drag arguments.

The present paper describes the first direct experimental test of these elements under a real shock acceleration and with real fluids. We describe shock-tube experiments in which a $M \approx 1.3$ shock wave crosses an initially perturbed interface from air to SF_6 . The initial perturbations that are reported include a single-mode perturbation, for studying the single-mode bubble and spike evolution, and an initial two-bubble shape perturbation, for studying the bubble-competition process. The experimental results are compared with full numerical simulations as well as the simple potential-flow model [3]. Even though in the present experiment these key elements of the bubble-merger model are tested for the shock acceleration case, its success strengthens the applicability of the model in a more general acceleration history such as in the RT case.

The experiments are performed in a 7.5 meter-long horizontal double-diaphragm shock tube with an $8 \text{ cm} \times 8 \text{ cm}$ cross section. A $0.1 \mu\text{m}$ nitrocelluloid membrane separates the two gases. To produce the initial perturbation, we stretch the membrane over thin copper wires mounted at different positions across the shock tube. The magnitude of the initial perturbation was large compared to the thickness of the membrane in order to minimize the effect of the membrane on the results. Experiments and simulations show that the exact shape and the impurity of the modes of the initial perturbation, caused by the number of wires which are used, has only minor influence on the late time nonlinear bubble and spike evolution. During the whole experiment rarefaction waves from the drive section are far behind the interaction region and the shock is steady. The evolution of the mixing region induced by the shock wave is measured in each experiment by photographing a series of schlieren pictures using a copper-vapor laser pulsed at a rate of about 10 kHz and a shutterless rotating prism camera. The experimental apparatus is described in more detail in Ref. [16].

Single-mode experiments.—Single-mode experiments were carried out with initial perturbation wavelengths of 80, 40, 26, and 16 mm, corresponding to wave numbers 1, 2, 3, and 5, respectively, with amplitude of 2 mm. Figure 1(a) shows a time evolution sequence of the $\lambda = 80 \text{ mm}$ case. During most of the experiment the perturbation amplitude is small enough so it can be expected to stay in the linear regime. However, for the $\lambda = 26 \text{ mm}$ case, Fig. 1(b), the perturbation has entered deep into the nonlinear stage.

In the first few frames of each case one can see the shock advancing ahead of the perturbed interface. Since

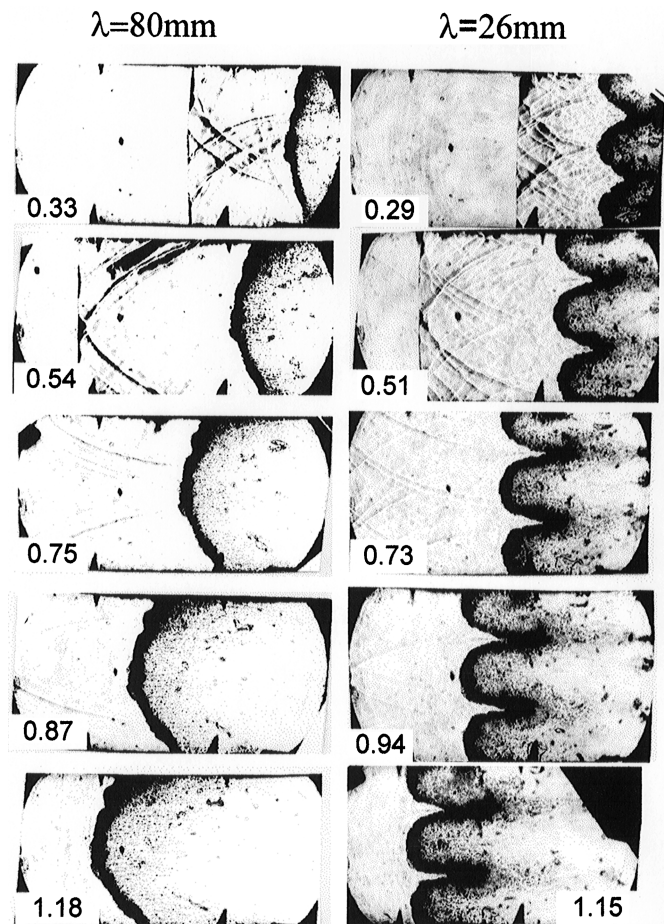


FIG. 1. Series of schlieren photographs from single $M = 1.3$ Air/ SF_6 experiment. Left column: $\lambda = 80 \text{ mm}$. Right column: $\lambda = 26 \text{ mm}$. Numbers indicate time after shock passage in msec.

we would like to infer the location of the bubble and spike front relative to the unperturbed interface, one has to measure the location of the unperturbed interface. The interface velocity is obtained from the measured shock velocity using the Rankine-Hugoniot equation. Figure 2 shows the evolution of the bubble and spike tips relative to the unperturbed interface. In order to put all the single-mode experiments on one unified graph, we have plotted in Fig. 2 the bubble and spike tip heights $h(t)$ in dimensionless units, $[h(t) - h(0)]k$, as a function of the dimensionless time, $U_0 kt$, with U_0 the Richtmyer initial velocity. Also plotted in Fig. 2 are the heights obtained from the analytical formula of Eq. (1) using $C = 1/3\pi$ (solid line) and $C = 1/2\pi$ (dashed line). It can be seen that the $C = 1/3\pi$ coefficient fits the experimental results better, as is expected for $A = 0.67$. The agreement is very good for the bubble front and reasonably good for the spike front, where the experimental error in determining the tip location is larger.

Similar experiments were conducted by other groups [17,18]. Of particular interest is that done by Aleshin *et al.* [18] using Xe and Ar as gases ($A = 0.53$) at

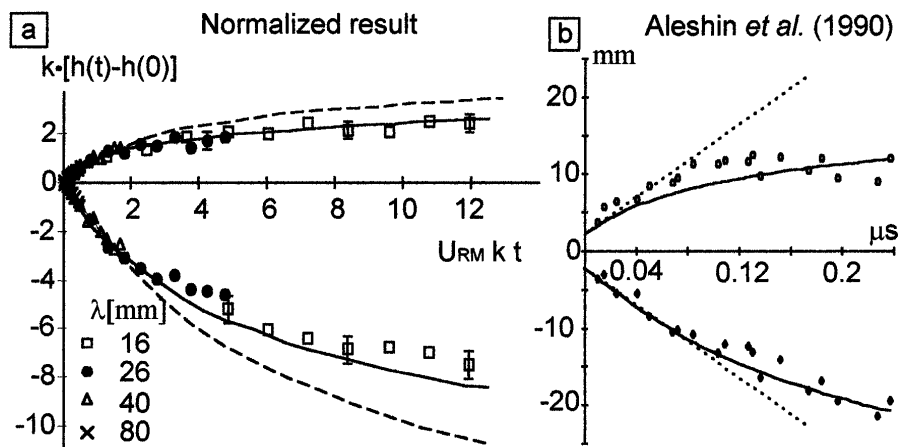


FIG. 2. Single mode bubble and spike evolution. (a) The present results. Heights are in normalized coordinates. The experimental error is mainly due to the uncertainty in the unperturbed interface position. (b) The experiment of Aleshin *et al.* [18] with $M = 3.5$ and $A = 0.53$. The lines in (a) are based on Eq. (1) with $C = \frac{1}{3}\pi$ (solid) and $\frac{1}{2}\pi$ (dashed). The lines in (b) are based on Eq. (1) with $\frac{1}{3}\pi$ (solid) and the linear growth (dashed).

a higher Mach number, $M = 3.5$, where compressible effects are more pronounced. Figure 2(b) compares the results of Aleshin *et al.* for $\lambda = 36$ mm (Fig. 3 in [18]) with our analytical formula with $C = 1/3\pi$ (solid line). The data in Aleshin's experiment are much more scattered than in our experiment, probably due to the fact that each pair of data points (bubble and spike) was recorded in a different experiment and that the interface location was inferred from a 1D simulation. The fact that the same formula, which is based on an incompressible theory, fits well both the weakly compressible case ($M = 1.3$) and the moderately compressible case ($M = 3.5$) suggests that the evolution of the RM instability after passage of the shock is determined mainly by incompressible effects. Future work will determine whether this also applies to the highly compressible case, such as the $M \approx 20$ experiment of Dimonte *et al.* [19].

Bubble-competition experiments.—We now turn to the two-bubble interaction experiments. We chose an array of alternating large (25–27 mm) and small (10–17 mm) bubbles for comparison with simulations which were done with a two-dimensional compressible ALE code with interface tracking [13] and the potential flow model of Hecht *et al.* [3]. The central part of the membrane always consisted of a small bubble flanked by two large bubbles, and the two sides were completed by partial small bubbles. The initial amplitudes of the large and small bubbles were chosen such that the initial velocities of both bubbles according to the Richtmyer formula were similar (i.e., $a_l/a_s = \lambda_l/\lambda_s$, where s and l are the small and large bubbles, respectively). Figure 3 shows the time evolution of the interface in a 27 mm/17 mm experiment. Superimposed on the experimental pictures is the interface structure from the full simulation results. The agreement between the experimental results and the numerical simulation is very good, including the change

in the small bubble location and size relative to the two large neighboring bubbles. The bubble-merger process can be seen from the shape of the small and large bubbles and especially from the orientation of the spikes between the larger and smaller bubbles, which skew toward the large bubbles as they overtake the small one.

The competition process is better seen by plotting the bubble tip locations relative to those measured and calculated for the single-mode case. In Fig. 4(a) we have plotted the two bubble heights for a 25 mm/10 mm experiment, relative to the unperturbed interface (dashed line). The figure shows the experimental results, the full

Bubble competition

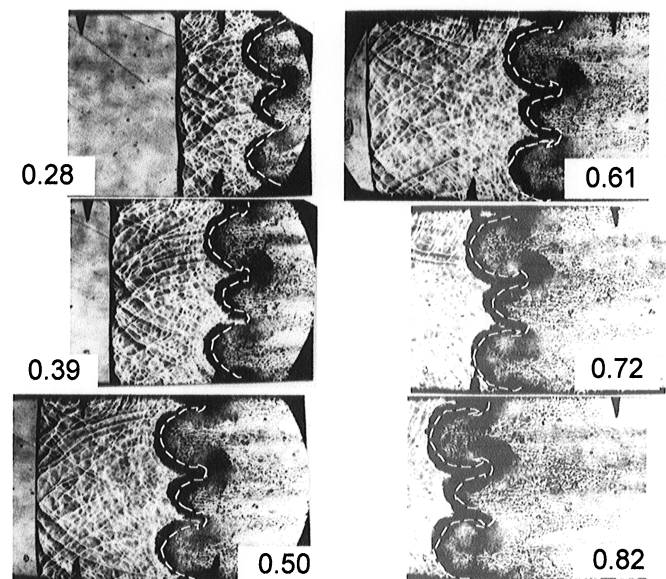


FIG. 3. The evolution of the interface for $M = 1.25$, $\lambda_1 = 27$ mm, $\lambda_2 = 17$ mm; simulation results: dashed line.

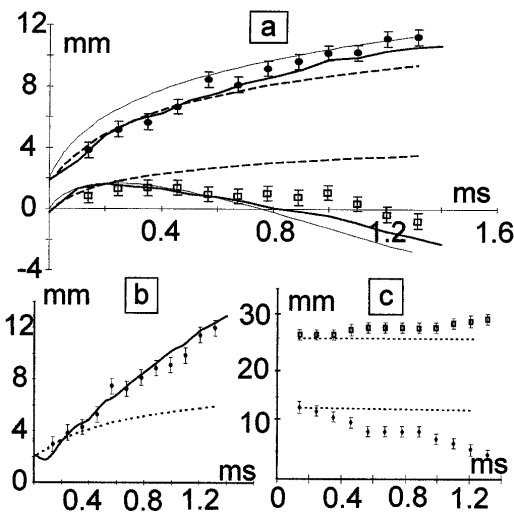


FIG. 4. Two-bubble experiment. (a) Bubble height in a 25 mm/10 mm experiment; experiment: dots; potential flow model: light line; full-scale simulation: heavy line; noninteracting bubble front growth dashed line. (b) Height difference between the tips of the two bubbles. (c) The bubble wavelength, defined by the maximum width of the large bubble.

numerical simulation (heavy line), and the potential flow model (light line). For the model we use the $A = 1$ description but with the initial bubble velocity taken from the Richtmyer formula, which includes the A dependence, and is the main A dependence of the process [2]. Also plotted are the two individual noninteracting bubble evolution lines, derived from Eq. (1), which was shown above to fit the single-mode bubble evolution very well (Fig. 2). Initially the two bubbles evolve according to the noninteracting lines, but in the nonlinear stage a strong interaction takes place, the result of which is the faster growth of the larger bubble and the shrinking of the smaller bubble downstream. The agreement between the full simulation, the simple potential flow model, and the experimental results is very good. The bubble competition is even more pronounced when one looks at the height difference between the tips of the two bubbles [Fig. 4(b)]. This provides an accurate experimental measurement since it is independent of the interface location. The rapid increase in the height difference compared to that of two noninteracting bubbles (dashed line) is clearly seen, demonstrating the bubble-merger process. The overtaking process can also be seen by measuring the widths of the two bubbles. Figure 4(c) shows the two bubble wavelengths inferred from the experimental data. The larger bubble clearly increases in width while the smaller bubble shrinks. It can be seen from all the measures shown in Figs. 4(a)–4(c) that the bubble-interaction process starts to be important at $t \approx 0.3$ msec.

In summary, we have performed the first experiments that clearly demonstrate the key elements of the bubble-merger model: the single-mode bubble and spike

evolution and the two-bubble interaction process. The experimental results were found to be in very good agreement with both the theoretical model and full numerical simulations, which were used to infer the evolution of a multimode initial perturbation for both the RM and RT instabilities. Further work will present the dependence of these elements on the fluid density ratio, the effect of a reshock on the perturbed interface, and the evolution of the mixing zone from a random initial perturbation.

- [1] J.D. Lindl, *Phys. Plasmas* **2**, 3933 (1995); S.W. Haan *et al.*, *Phys. Plasmas* **2**, 2480 (1995); J.D. Kilkenny *et al.*, *Phys. Plasmas* **1**, 1379 (1994); B.A. Remington *et al.*, *Phys. Fluids B* **5**, 2589 (1993).
- [2] U. Alon, J. Hecht, D. Mukamel, and D. Shvarts, *Phys. Rev. Lett.* **72**, 2867 (1994); U. Alon, J. Hecht, D. Ofer, and D. Shvarts, *Phys. Rev. Lett.* **74**, 534 (1995).
- [3] J. Hecht, U. Alon, and D. Shvarts, *Phys. Fluids* **6**, 4019 (1994).
- [4] Q. Zhang and S.-I. Sohn, *Phys. Lett. A* **212**, 149 (1996); *Phys. Fluids* **9**, 1106 (1997).
- [5] Y. Yang, Q. Zhang, and D.H. Sharp, *Phys. Fluids* **6**, 1856 (1994).
- [6] R.D. Richtmyer, *Commun. Pure Appl. Math.* **13**, 297 (1960).
- [7] J.W. Grove, R. Holmes, D.H. Sharp, Y. Yang, and Q. Zhang, *Phys. Rev. Lett.* **71**, 3473 (1993).
- [8] S.W. Haan, *Phys. Rev. A* **39**, 5812 (1989); *Phys. Fluids B* **3**, 2349 (1991).
- [9] H.J. Kull, *Phys. Rev. A* **33**, 1957 (1986).
- [10] J.W. Jacobs and J.M. Sheeley, *Phys. Fluids* **8**, 405 (1996); N. Zabusky, J. Ray, and S. Samtany, in *The Proceedings of the 5th International Workshop on Compressible Turbulent Mixing, Stony Brook, 1995*, edited by R. Young, J. Glimm, and B. Boston (World Scientific, Singapore, 1996), p. 89; A. Rikanati (private communication).
- [11] R. Clift, J.R. Grace, and M.E. Weder, *Bubbles, Drops and Particles* (Academic Press, New York, 1978).
- [12] D. Shvarts, U. Alon, D. Ofer, R.C. McCrory, and C.P. Verdon, *Phys. Plasmas* **2**, 2465 (1995).
- [13] D. Ofer, U. Alon, D. Shvarts, R.L. McCrory, and C.P. Verdon, *Phys. Plasmas* **3**, 3073 (1996).
- [14] B.A. Remington *et al.*, *Phys. Plasmas* **2**, 241 (1995).
- [15] D.H. Sharp, *Physica (Amsterdam)* **12D**, 3 (1984); C.L. Gardner, J. Glimm, O. McBryan, R. Menikoff, D.H. Sharp, and Q. Zhang, *Phys. Fluids* **31**, 447 (1988); J. Glimm, X.R. Li, R. Menikoff, D.H. Sharp, and Q. Zhang, *Phys. Fluids A* **2**, 2046 (1990).
- [16] L. Erez, O. Sadot, G. Erez, and L.A. Levin, in *The Proceedings of the 5th International Workshop on Compressible Turbulent Mixing, Stony Brook, 1995* (Ref. [10]), p. 169.
- [17] R. Benjamin, D. Besnard, and J. Haas, LANL Report No. LA-UR 92-1185, 1993.
- [18] A.N. Aleshin, E.V. Lazareva, S.G. Zaitsev, V.B. Rozanov, E.G. Gamali, and I.G. Lebo, *Sov. Phys. Dokl.* **35**, 159 (1990).
- [19] G. Dimonte, C.E. Frerking, M. Schneider, and B.A. Remington, *Phys. Plasmas* **3**, 614 (1996).